



**AUSTRALIAN NUCLEAR SCIENCE  
AND TECHNOLOGY ORGANISATION**

**LUCAS HEIGHTS RESEARCH LABORATORIES**

**NEUTRON TRANSMUTATION DOPING OF SILICON  
FOR THE PRODUCTION OF RADIATION DETECTORS**

by

**D. ALEXIEV**

**NOVEMBER 1987**

**ISBN 0 642 59871 1**

AUSTRALIAN NUCLEAR SCIENCE  
AND TECHNOLOGY ORGANISATION

LUCAS HEIGHTS RESEARCH LABORATORIES

NEUTRON TRANSMUTATION DOPING OF SILICON  
FOR THE PRODUCTION OF RADIATION DETECTORS

by

D. ALEXIEV

ABSTRACT

P-type silicon was doped by neutron transmutation (NTD-Si) to produce high resistivity n-type silicon suitable for the production of surface barrier radiation detectors. Deep level transient spectroscopy (DLTS) analysis showed no remnant traps following annealing (850°C) of the NTD-Si in the presence of a phospho-silicate glass getter. Surface barrier radiation detectors constructed from this material showed no significant charge trapping and compare favourably with those constructed of float-zone (FZ) Si.

National Library of Australia card number and ISBN 0 642 59871 1

The following descriptors have been selected from the INIS Thesaurus to describe the subject content of this report for information retrieval purposes. For further details please refer to IAEA-INIS-12 (INIS: Manual for Indexing) and IAEA-INIS-13 (INIS: Thesaurus) published in Vienna by the International Atomic Energy Agency.

ANNEALING; CRYSTAL DOPING; ELECTRIC CONDUCTIVITY; IRRADIATION; NEUTRONS; SILICON;  
SURFACE BARRIER DETECTORS

#### EDITORIAL NOTE

From 27 April 1987, the Australian Atomic Energy Commission (AAEC) is replaced by Australian Nuclear Science and Technology Organisation (ANSTO). Serial numbers for reports with an issue date after April 1987 have the prefix ANSTO with no change of the symbol (E, M, S or C) or numbering sequence.

## CONTENTS

1. INTRODUCTION	1
2. EXPERIMENTAL	2
2.1 Sample Preparation	2
2.2 Neutron Irradiation	3
3. SILICON OBTAINED FROM OTHER SUPPLIERS	4
4. EVALUATION OF HIGH RESISTIVITY NTD-SILICON	5
5. CONCLUSIONS	5
6. ACKNOWLEDGEMENTS	5
7. REFERENCES	5

Figure 1	General sequence used in the NTD process on a Si wafer	7
Figure 2	The radial acceptor variation along two axes of a 30 mm $\phi$ Si (p-type) wafer	7
Figure 3	Model of flow pattern and dopant concentration profile in float-zone silicon growth	8
Figure 4	Gamma-ray spectra of the residual activity taken three days after irradiation	8
Figure 5	Fluence, $\Phi$ ( $\text{n cm}^{-2}$ ), v. $N_D$ and $N_A$ ; also shown is the starting point based on the W-profile found earlier ( $N_A = 0.9$ and $1.0 \times 10^{13} \text{ cm}^{-3}$ )	9
Figure 6	$N_D$ and $N_A$ v. fluence showing that group 4 is n-type and compensated with an $N_D$ from $8 \times 10^{10}$ to $5 \times 10^{11} \text{ cm}^{-3}$	9
Figure 7	Reverse current characteristics of an NTD-Si radiation detector	10
Figure 8	Residual donor distribution in an NTD-Si radiation detector diode measured to a depth of 1000 $\mu\text{m}$	10
Figure 9	An americium-241 spectrum produced by an NTD-Si surface barrier detector	11
Figure 10	Residual radioactivity in the bulk of the NTD-Si detector	11

## 1. INTRODUCTION

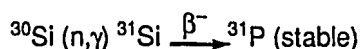
When constructing high quality Si surface barrier radiation detectors, especially guarded structures for X-ray spectrometers, the main requirements are first that the material has to be n-type, doped with the donor phosphorus and second that it is of high resistivity (of the order of 50 k $\Omega$ .cm or greater) with a good degree of uniformity. Such material is derived from conventional float-zone (FZ) crystal growth methods but is expensive and difficult to obtain.

To produce high resistivity n-type Si, the residual phosphorus impurity has to be critically controlled during the growth phase of the crystal. Added to this problem, phosphorus has a high vapour pressure, thereby dissociating from the crystal surface at high temperature. Phosphorus also has a segregation coefficient less than unity ( $C_{\text{solid}}/C_{\text{liquid}} = 0.35$ ) and therefore the uptake of the phosphorus atom is directly dependent on the temperature gradient at the Si solidus. Any variations in the doping density result in poor uniformity of the resistivity of the crystal. Typically, radial variations have a W-profile with a resistivity change of up to 20 per cent. For this reason, prior to neutron transmutation doping (NTD), it is important to select regions of uniform resistivity. This can be achieved by characterising large area sections and discarding the edge and centre region. A second consideration should be the examination of Si produced by various commercial suppliers for lowest resistivity variations.

Uniformly doped high resistivity n-type Si has been produced by the NTD process and has been demonstrated by Haas and Schnoeller [1976], Kim *et al.* [1979] and von Ammon and Kemmer [1984] to be as good as that produced by FZ methods. The radiation damage produced by the neutron-Si lattice interaction can be removed by annealing [Malmros 1978] and the residual radioactivity of the transmuted Si is almost negligible, except for low background applications.

### Production of donor atoms in Si by NTD

Doping reaction:



$^{30}\text{Si}$ : 3.08% isotopic abundance

$^{31}\text{Si}$ : 2.6 h half-life

$\sigma(n, \gamma)$ : 0.13 barn

The starting material for the NTD process is p-type Si which has had most of the phosphorus residual impurity removed by repeated zone-refining passes, leaving boron, an acceptor, as a residual impurity uniformly distributed throughout the crystal. Boron is known to have a low vapour pressure and a segregation coefficient nearly equal to unity. However, the level of the boron should be low, as large neutron fluences ( $\Phi$ ) would be required to counter-dope the Si, with the danger of over-compensation turning the p-type Si into an n-type Si of similar resistivity. For example, a net acceptor level ( $N_A$ ) of  $10^{13} \text{ cm}^{-3}$  would require a neutron fluence in the order of  $10^{17} \text{ n cm}^{-2}$  for total compensation. Therefore if a final donor level ( $N_D$ ) of  $10^{10} \text{ cm}^{-3}$  is aimed for, a fluency control of one part in 1000 has to be achieved. Such control over the NTD process could only be attempted incrementally with repeated measurements of the changing  $N_A$  level.

Thus the aim will be to NTD treat p-type Si in a controlled, step-wise fashion to produce high resistivity, of the order of 100 k $\Omega$ .cm, in an n-type crystal.

It is also interesting to note that if the Si crystal is produced by the decomposition of monosilane, very small quantities of boron will be present in the crystal as the production of the source gas  $\text{SiH}_4$  involves an associated reaction producing boron hydride [Yusa *et al.* 1975], leaving the  $\text{SiH}_4$  virtually clean of boron. If other source gases, such as  $\text{SiHCl}_3$  or  $\text{SiCl}_4$  are used, boron levels tend to be higher [Yusa *et al.* 1975].

## 2. EXPERIMENTAL

### 2.1 Sample Preparation

A 30 mm diameter, 74 mm long section of 1400-2600  $\Omega \cdot \text{cm}$  p-type Si, grown in the  $\langle 111 \rangle$  direction, was obtained from TOPSIL. Two wafers, 2 mm and 7 mm thick, were cut, lapped and etched in  $4\text{HNO}_3:1\text{HF}$  for ten minutes. All initial measurements and NTD treatment were first done on the 2 mm thick wafer as a basis for the rest of the material.

Actual resistivity fluctuations have been noted by a number of workers, and in particular by von Ammon and Kemmer [1984] for both p- and n-type Si in the  $\langle 100 \rangle$  and  $\langle 111 \rangle$  orientations. They suggested that when such material is highly compensated, the difference in profiles can lead to p-n junction formation across the wafer. For this reason the distribution of the acceptor ( $N_A$ ) has to be measured across the wafer, and can best be achieved by building a series of diode structures in a cross-formation as shown in figure 1a. As the material is p-type, the rectifying contact is Al and the ohmic contact Au. A series of measurements to a depletion depth of 45  $\mu\text{m}$  was made for each diode. Figure 2 shows the radial acceptor variation for depletion depths of 20 and 35  $\mu\text{m}$  for two axes.

It can be noted from figure 2 that the acceptor level varies by up to ten per cent across the full diameter of the wafer in a W-shaped profile. This shape is not surprising when considering the variation of the dopant concentration during the float-zone (FZ) crystal growth process. Glasow and Kolbesen [1983] described a flow torus forming in the melt zone above certain rotational speeds of the crystal seed. This results in stagnation regions in the centre and periphery of the melt forming a thick diffusion layer. A thin diffusion layer is formed in between. The dopant concentration will vary accordingly, resulting in a W-shaped concentration profile. A model of float-zone crystal growth and its dopant concentration profile are shown in figure 3.

However, despite finding such a radial variation, and realising that it would be detrimental to conclusive results, as the compensation tolerance is of the order of one part in 1000, the wafer was cut into four segments (figure 1b). The Al and Au were stripped with a series of etches. Dilute HF was used to remove the Al, and  $3\text{HCl}:1\text{HNO}_3$  to remove the Au, followed by three two-minute etches in  $4\text{HNO}_3:1\text{HF}$ . The segments were finally etched in a solution of  $8\text{H}_2\text{O}:1\text{HCl}:1\text{H}_2\text{O}_2$  at  $60^\circ\text{C}$  for 11 minutes, thereby ensuring that all traces of Au had been removed. The segments of Si were then sealed in polythene and submitted for neutron irradiation in the reactor HIFAR, a 10 MW DIDO class research reactor located at Lucas Heights, Australia. All irradiations were done in RIG X7, 'B' position, and rated at  $\sim 4 \times 10^{12} \text{ n cm}^{-2} \text{ s}^{-1}$ .

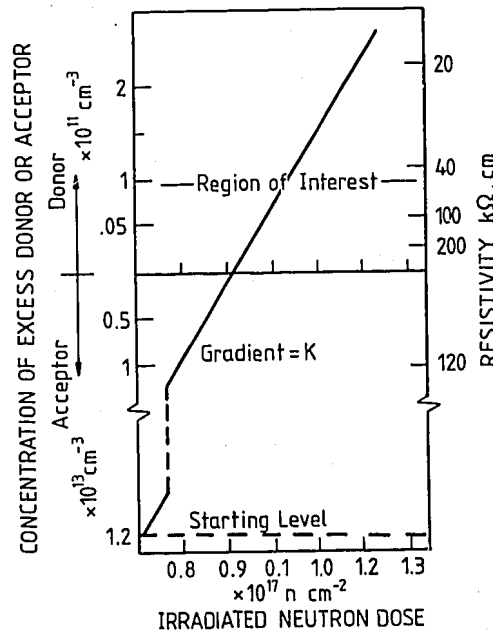
The relationship between generated donor concentration and neutron fluence can be estimated firstly from the initial  $N_A$  finding (figure 2) and the simple linear relationship expressed by

$$\begin{aligned} \Delta N &= N(^{31}\text{P}) - N_A \\ &= K \Phi - N_A \end{aligned}$$

where K is the transmutation constant (atom/neutron cm) and the irradiation dose,  $\Phi$ , is given by

$$\Phi = \phi t \text{ (neutrons cm}^{-2}\text{)}.$$

Representing this relationship schematically,



Using published data for  $K = 1.7 \times 10^{-4}$  atom/n cm [Klm *et al.* 1979], an irradiation sequence can be set up.

Sample:	1	for	$N = 0.5 \times 10^{13} \text{ cm}^{-3}$ requires $\Phi = 0.88 \times 10^{17} \text{ n cm}^{-2}$
	2		$N = 0.75 \times 10^{13} \text{ cm}^{-3}$ requires $\Phi = 1.03 \times 10^{17} \text{ n cm}^{-2}$
	3		$N = 0.9 \times 10^{13} \text{ cm}^{-3}$ requires $\Phi = 1.118 \times 10^{17} \text{ n cm}^{-2}$
	4		$N = 1 \times 10^{13} \text{ cm}^{-3}$ requires $\Phi = 1.18 \times 10^{17} \text{ n cm}^{-2}$

Thus, after annealing and rebuilding a new series of diode structures as shown in **figure 1c**, new values for  $N_A$  and the transmutation constant  $K$  could be calculated.

## 2.2 Neutron Irradiation

The four samples of group 1 were prepared as described above and submitted to the HIFAR irradiation facility. After irradiation, a minimum period of three days to one week was allowed to elapse so that the induced radioactivity was below the internationally acceptable standard for the removal and transport of packages as set in IAEA Safety Series No. 6 [IAEA 1985].

As the sealed polythene pouches in which the Si was irradiated were found to have some surface contamination, the Si samples were carefully removed and the pouches discarded at the irradiation facility, thereby ensuring that no loose active contamination was carried over to clean areas. The NTD-Si samples were then prepared for thermal annealing by dip etching in  $4\text{HNO}_3:1\text{HF}$  followed by a rinse in  $18 \text{ M}\Omega \text{ H}_2\text{O}$ . The residual radioactivity of the NTD-Si was then measured with a  $\text{Ge(Li)}$  detector. The  $\gamma$ -ray spectrum (**figure 4a**) showed an  $^{198}\text{Au}$  photo-peak, indicating Au contamination on the Si surface, possibly caused by replating of the Au metallisation during the etch, or by remnants of Au impurities found in HF. After the final etch ( $8\text{H}_2\text{O}:1\text{HCl}:1\text{H}_2\text{O}_2$  at  $60^\circ \text{C}$  for 11 minutes) the Au photo-peak disappeared (**figure 4b**). Such  $\gamma$ -ray spectroscopic analyses were adopted for all samples before thermal annealing, thereby avoiding Au diffusion into the Si.

Before thermal annealing, all Si samples were covered on both faces with a getter (a solution of  $\text{P}_2\text{O}_5$  in 2-butoxy ethanol) and placed, in a wet condition, into a quartz tube and located in a controlled furnace. The thermal annealing took place at  $850^\circ\text{C}$  for two hours in air. Power to the furnace was then switched off and, after a period of eight hours, which was the thermal time constant of the furnace, the samples were removed. The getter (now a glass of some  $100 \mu\text{m}$ ) was removed by etching in HF for four minutes, followed by dip etching in  $4\text{HNO}_3:1\text{HF}$  and quenching in  $18 \text{ M}\Omega \text{ H}_2\text{O}$ . The Au barrier and Al ohmic contact were then evaporated.

A series of capacitance-voltage (C-V) measurements produced the following  $N_D$  values:

Group	Sample	$N_D (\text{cm}^{-3})$	$\Phi (\text{n cm}^{-2})$
1	1	$0.615 \times 10^{13}$	$0.88 \times 10^{17}$
	2	$0.91 \times 10^{13}$	$1.03 \times 10^{17}$
	3	$0.965 \times 10^{13}$	$1.118 \times 10^{17}$
	4	$1.07 \times 10^{13}$	$1.18 \times 10^{17}$

The results indicate that the Si is n-type, but over-compensated at an  $N_D$  level not suitable for device (detector) construction. However, the transmutation constant  $K$  can be calculated from this data and the  $N_A$  values in the W profile (**figure 2**):  $K_{\text{max}} = 1.696 \times 10^{-4}$ ,  $K_{\text{min}} = 1.612 \times 10^{-4}$  (**figure 5**).

Based on these findings, three more groups were irradiated and treated similarly with the following results:

Group	Sample		$N(x) \text{ (cm}^{-3}\text{)}$	$\Phi \text{ (n cm}^{-2} \times 10^{16}\text{)}$
2	1	$N_A$	$1.65 \times 10^{12}$	4.8
	2		$1.35 \times 10^{12}$	5.0
	3		$0.8 \times 10^{12}$	5.4
	4		$0.75 \times 10^{12}$	5.5
3	1	$N_D$	$8 \times 10^{10} - 8 \times 10^{11}$	5.8
	2		$2 \times 10^{12}$	6.2
	3		$3.2 \times 10^{12}$	6.5
	4		$2 \times 10^{12}$	6.8
4	1	$N_A$	$1 \times 10^{11}$	5.55
	2		$1 \times 10^{11}$	5.60
	3		$2 \times 10^{11}$	5.70
	4		$2 \times 10^{11}$	5.75

A plot of  $N_A$  and  $N_D$  versus  $\Phi$  is shown in figure 5. A DLTS run for each group showed no NTD-induced deep levels left after the thermal annealing process. The material remained free of electrically active defects.

Silicon samples belonging to group 4 demonstrated that high resistivity ( $\sim 60 \text{ k}\Omega\text{.cm}$ ) n-type material can be produced by the NTD process. Subsequently, NTD-Si yielded  $\sim 100 \text{ k}\Omega\text{.cm}$  n-type material. The method is simple in nature when compared with the difficulties and costs involved in the production of FZ Si in the  $100 \text{ k}\Omega\text{.cm}$  range.

The scatter in figure 6 can be explained by variations in the neutron flux (RIG X7 is rated at  $\pm 5\%$  of  $2.4 \times 10^{12} \text{ n cm}^{-2} \text{ s}^{-1}$ ) and in the timing procedure of the facility. It is interesting to note that such problems can be eliminated [Gunn *et al.* 1978] by using rhodium wire detectors (Reuter Stokes, Cleveland, Ohio) combined with analogue current integrators and pre-set alarms. The neutron detector utilises the  $\beta$ -decay of  $^{104}\text{Rh}$  to produce a current proportional to the neutron flux. Thus in a similar way to  $\Phi$  versus  $N(x)$ , charge versus  $N(x)$  calibration constants could be obtained, reducing the NTD process to a routine level by eliminating progressive  $N_A$  or  $N_D$  measurement and fluence readjustment.

### 3. SILICON OBTAINED FROM OTHER SUPPLIERS

**Supplier No 1:** A 40 mm diameter section of p-type Si grown in the  $\langle 111 \rangle$  direction and of  $2.5 \text{ k}\Omega\text{.cm}$  resistivity, was processed as described earlier. The acceptor ( $N_A$ ) profile was found to vary 45 per cent from the edge to the centre having the shape of an inverted U. A DLT spectrum showed a minority trap, located at 300 K ( $\tau_c = 10 \text{ ms}$ ). After NTD treatment the relative intensity of this trap increased considerably and an additional majority trap was also noted.

**Supplier No 2:** This material was produced by the decomposition of monosilane with a resistivity of the order of  $10\text{-}15 \text{ k}\Omega\text{.cm}$ . The  $N_A$  distribution showed a typical W profile with a 15 per cent variation of the acceptor. DLTS analysis showed two minority traps located at 190 K and 300 K ( $\tau_c = 10 \text{ ms}$ ).

A second ingot from the same manufacturer had a flat profile where the  $N_A$  level was found to vary from the edge to a dip in the centre by seven per cent. However, again a DLT spectrum revealed a dominant minority trap at 270 K ( $\tau_c = 10 \text{ ms}$ ) which, after NTD, increased in intensity to an unusable level.

Attempts to construct a surface barrier detector failed owing to abnormal C-V characteristics and materials from suppliers 1 and 2 were abandoned.



#### 4. EVALUATION OF HIGH RESISTIVITY NTD-SILICON

The best way to evaluate the high resistivity NTD-Si is to construct a simple radiation detector. For this purpose material from group 4 was used, being n-type and compensated to a net donor level of  $N_D \sim 1 \times 10^{11} \text{ cm}^{-3}$ . The Si sections selected had a thickness of 1.5 mm. Constructing a radiation detector (diode) involved evaporating a  $0.363 \text{ cm}^2$  Au barrier on the opposite face to the diffused Li(n<sup>+</sup>) contact. Commonly Al is used to form an ohmic contact; however, as there is a possibility of forming non-ohmic regions when using high resistivity material, Li is diffused to a depth of  $\sim 300 \mu\text{m}$  followed by nickel plating of the diffused area. The method used to produce the n<sup>+</sup> contact closely followed that outlined by Beech and Eberhardt [1973]. After construction, the Si radiation detector was mounted in a holder and installed in an  $\ell\text{N}_2$  cryostat as part of an X-ray spectrometer system.

The reverse current characteristics of the diode are shown in figure 7 with a total leakage current of  $6 \times 10^{-12} \text{ A}$  at 100 volts. A C-V measurement taken at  $\ell\text{N}_2$  gave a residual  $N_D$  distribution (figure 8) at an average of  $1.5 \times 10^{11} \text{ cm}^{-3}$  to a depletion depth of  $800 \mu\text{m}$ . The sharp rise ( $N_D > 10^{12} \text{ cm}^{-3}$ ) in the  $N_D$  distribution at about  $900 \mu\text{m}$  depletion depth is the diffused Li(n<sup>+</sup>) contact.

An  $^{241}\text{Am}$  spectrum was accumulated over a period of 1000 s (figure 9) with a resolution of 650 eV FWHM on the 59.5 keV  $\gamma$ -ray line. A further measurement with a pulser set to an equivalent energy of 49.5 keV indicated that the resolution spread was mostly due to the ambient electrical noise level of the system and no contributing noise factor was generated by the NTD-Si detector.

A test was made for possible residual radioactivity present in the bulk of the detector four weeks after NTD irradiation. A spectrum (with no radioactive sources in the same room), taken over a period of four hours (figure 10) at an energy scale up to 70 keV, showed almost negligible background effects.

#### 5. CONCLUSIONS

The results obtained with NTD treatment of p-type Si showed that high quality material can be produced relatively simply and therefore economically. In the experiments  $1.2 \text{ k}\Omega\cdot\text{cm}$  p-type Si was compensated to n-type Si of the order of  $100 \text{ k}\Omega\cdot\text{cm}$ . The material after annealing had no significant induced trapping levels. Radiation detectors constructed out of the NTD-Si produced no charge trapping, usually seen as a non-Gaussian distribution of a photo peak, and generated no additional noise to a resolution of 650 eV FWHM  $^{241}\text{Am}$  spectrum. Recently, Bischoff [1985] has reported a resolution of 300 eV FWHM  $^{55}\text{Fe}$ , Mn K $\alpha$  line.

The results confirm that detectors made of NTD-Si have an important future in X-ray fluorescence spectrometry,  $\alpha$ -particle spectrometry and counting. It has also been shown that the residual radioactivity of isotopes, which may be present in the Si as inactive electrical impurities, seems to have a negligible effect on the performance of the detectors produced.

#### 6. ACKNOWLEDGEMENTS

I would like to thank Dr A J Tavendale for his continued interest and support of this work. I also thank Mr T Kluss and Mr J Wood for neutron irradiation of my samples and to Mr A A Williams for checking some of the detectors using DLTS.

#### 7. REFERENCES

- Beech, A. McG., and Eberhardt, J.E. [1973] - Semiconductor X-ray spectrometer system type 454. AAEC/E297.
- Bischoff, L. [1985] - Use of neutron-doped silicon in semiconductor detectors. *Sov. Phys.-Semicond. (Engl. Transl.)*, 19 (12), 1305-1307.
- Glasow, P.A., Kolbesen, B.O. [1983] - *Materials Research Society Symposia Proceedings*, Vol. 16. Elsevier Science, New York, p.17.
- Gunn, S.L., Meese, J.M., Alger, D.M. [1978] - Neutron Transmutation Doping in Semiconductors (Ed. J.M. Meese), Plenum Press, New York, p.197.
- Haas, W.E., Schnoeller, M.S. [1976] - Silicon doping by nuclear transmutation. *J. Electron. Mater.*, 5 (1), 57-68.

IAEA [1985] - Regulations for the safe transport of radioactive materials. *IAEA Safety Series*, No. 6. International Atomic Energy Agency, Vienna.

Kim, C., Kim, H., Yusa, A., Miki, S., Husimi, K., Ohkawa, S., Fuchi, Y. [1979] - High resistivity n-type silicon detectors produced by neutron transmutation doping. *IEEE Trans. Nucl. Sci.*, NS 26-1, 292.

Malmros, O. [1978] - Neutron Transmutation Doping in Semiconductors (Ed. J.M. Meese), Plenum Press, New York, p.249.

von Ammon, W., Kemmer, J. [1984] - Semiconductor processing. ASTM STP850.

Yusa, A., Yatsurugi, Y., Takaishi, T. [1975] - Ultrahigh purification of silane for semiconductor silicon. *J. Electrochem. Soc.*, 122 (12) 1700-1705.

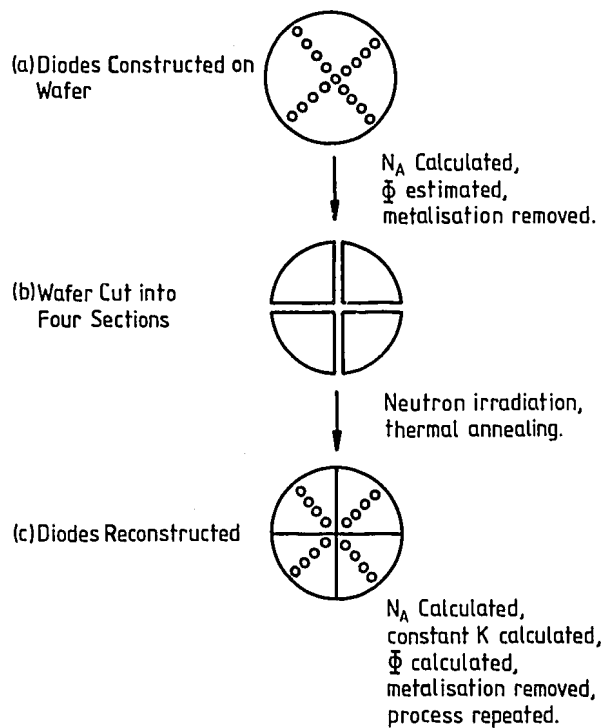


Figure 1 General sequence used in the NTD process on a Si wafer.

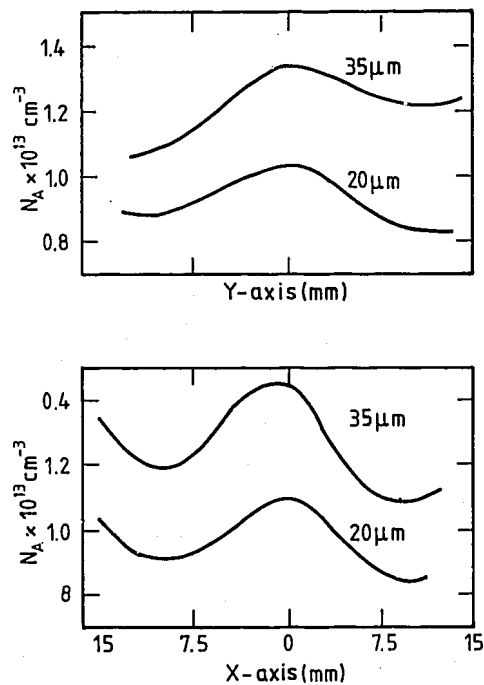


Figure 2 The radial acceptor variation along two axes of a 30 mm  $\phi$  Si (p-type) wafer.  $N_A$  measurements were done at 20 and 30  $\mu$ m depletion depths and are necessary for initial neutron fluence estimation.

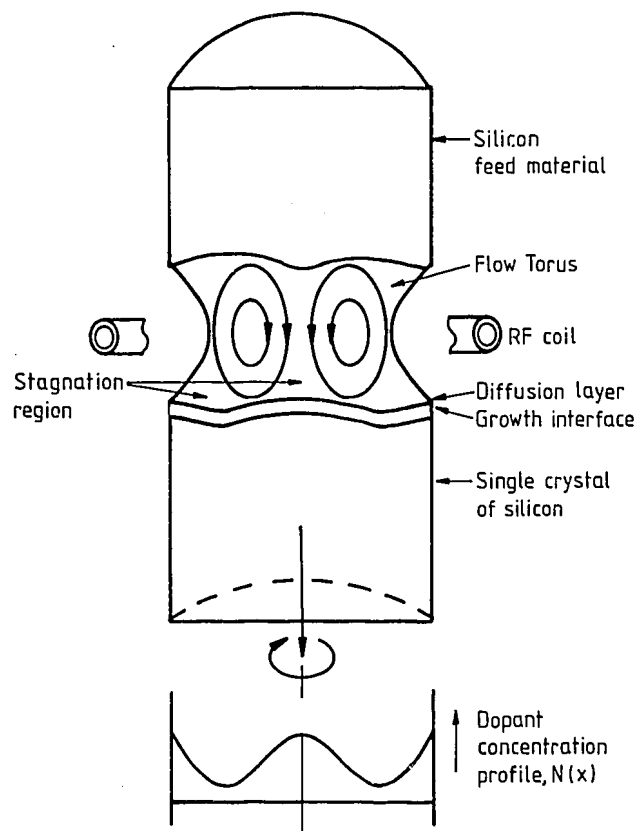


Figure 3 Model of flow pattern and dopant concentration profile in float-zone silicon growth

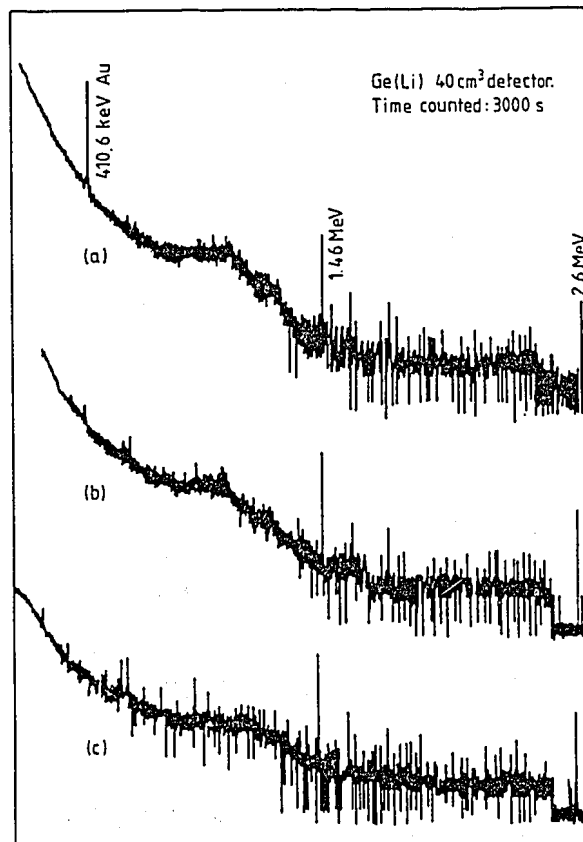


Figure 4 Gamma-ray spectra of the residual activity taken three days after irradiation: (a)  $^{198}\text{Au}$  photo-peak indicating Au contamination, (b) a further etch removed the Au, (c) background spectrum indicating that the 1.46 and 2.6 MeV lines are not in the NTD-Si.

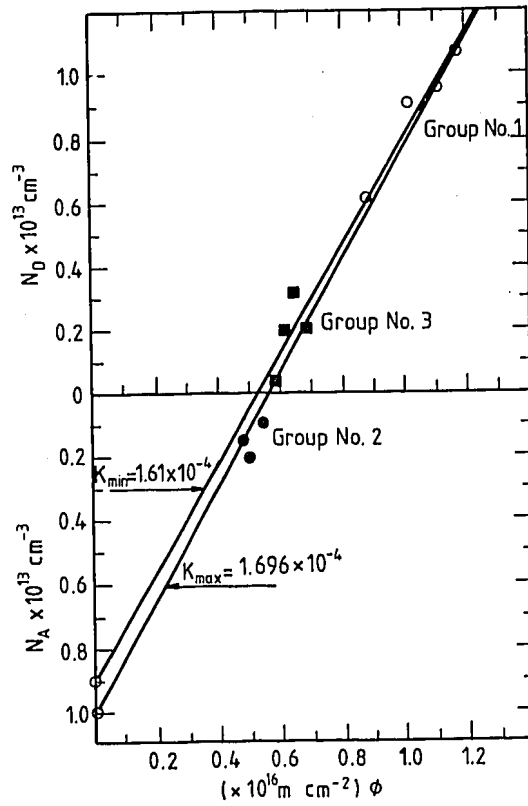


Figure 5 Fluence,  $\Phi$  ( $n \text{ cm}^{-2}$ ), v.  $N_D$  and  $N_A$ ; also shown is the starting point based on the W-profile found earlier ( $N_A = 0.9$  and  $1.0 \times 10^{13} \text{ cm}^{-3}$ )

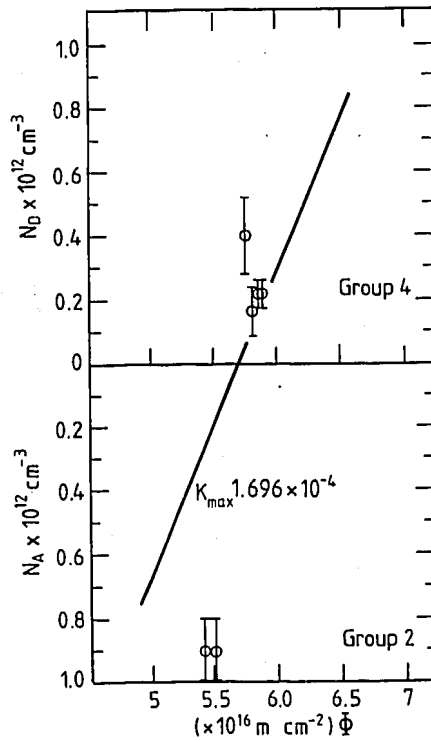


Figure 6  $N_D$  and  $N_A$  v. fluence showing that group 4 is n-type and compensated with an  $N_D$  from  $8 \times 10^{10}$  to  $5 \times 10^{11} \text{ cm}^{-3}$

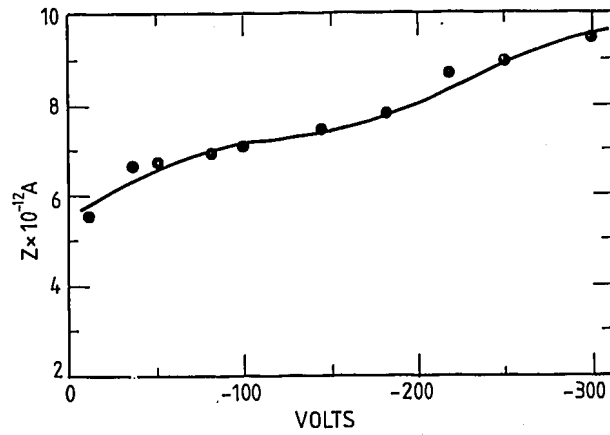


Figure 7 Reverse current characteristics of an NTD-Si radiation detector

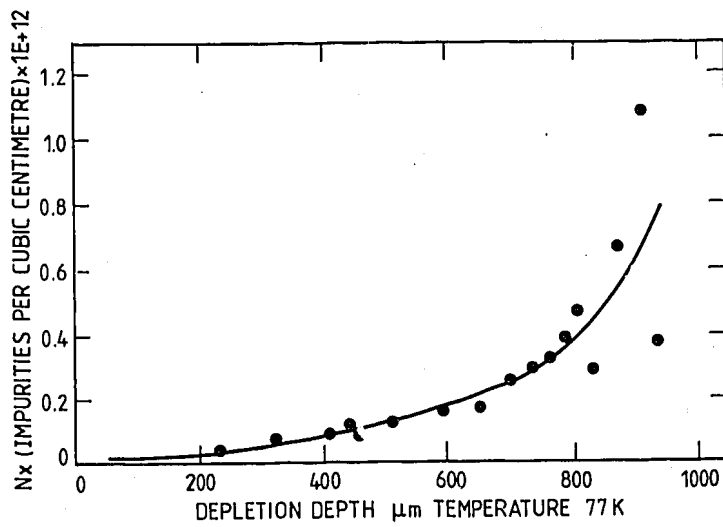


Figure 8 Residual donor distribution in an NTD-Si radiation detector diode measured to a depth of 1000  $\mu\text{m}$

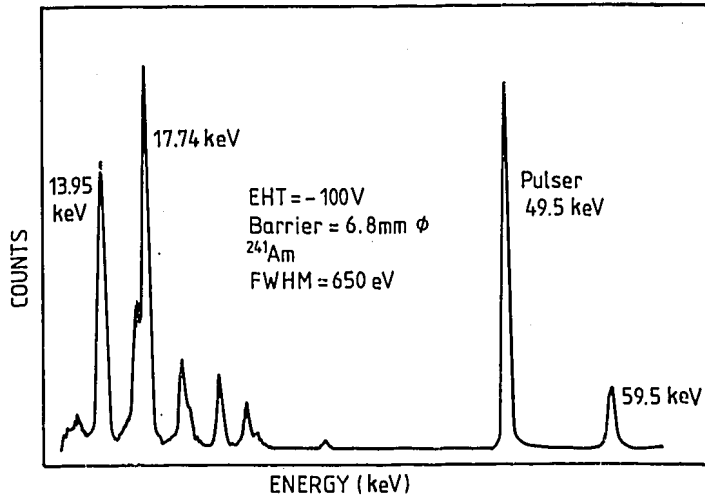


Figure 9 An americium-241 spectrum produced by an NTD-Si surface barrier detector

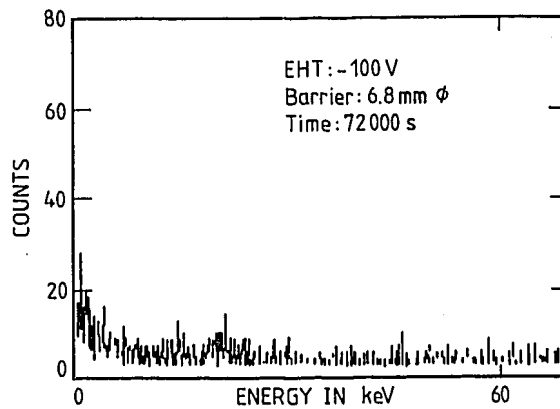


Figure 10 Residual radioactivity in the bulk of the NTD-Si detector